

Investigating exotic heavy-light tetraquarks with 2 + 1 flavour lattice QCD

Brian Colquhoun,^{a,*} Anthony Francis,^b Renwick J. Hudspith,^c Randy Lewis^a and Kim Maltman^{d,e}

^a*Department of Physics and Astronomy, York University,
Toronto, Ontario, M3J 1P3, Canada*

^b*Albert Einstein Center, Universität Bern,
CH-3012 Bern, Switzerland*

^c*PRISMA⁺ Cluster of Excellence & Institut für Kernphysik,
Johannes Gutenberg-Universität Mainz, D-55099 Mainz, Germany*

^d*Department of Mathematics and Statistics, York University,
Toronto, Ontario, M3J 1P3, Canada*

^e*CSSM, University of Adelaide,
Adelaide, SA, 5005, Australia*

*E-mail: bcolqu@yorku.ca, afrancis@itp.unibe.ch,
renwick.james.hudspith@gmail.com, randy.lewis@yorku.ca, kmaltman@yorku.ca*

There are a number of tetraquark channels for which some phenomenological models – already constrained by the ordinary meson and baryon spectrum – predict deep binding. We present results from our lattice calculations of doubly-charmed and bottom-charm channels where such predictions exist. Finding no evidence of deep binding, we can rule out those models, although this does not preclude the possibility of shallow binding for those states. On the other hand, a consistent picture of deeply-bound, strong-interaction stable $I = 0$, $J^P = 1^+ ud\bar{b}\bar{b}$ and $I = 1/2$, $J^P = 1^+ \ell s\bar{b}\bar{b}$ (with $\ell = u/d$) tetraquarks has emerged from lattice studies over the last few years. We discuss the results of our calculations in each of these channels.

*The 38th International Symposium on Lattice Field Theory, LATTICE2021 26th-30th July, 2021
Zoom/Gather@Massachusetts Institute of Technology*

*Speaker

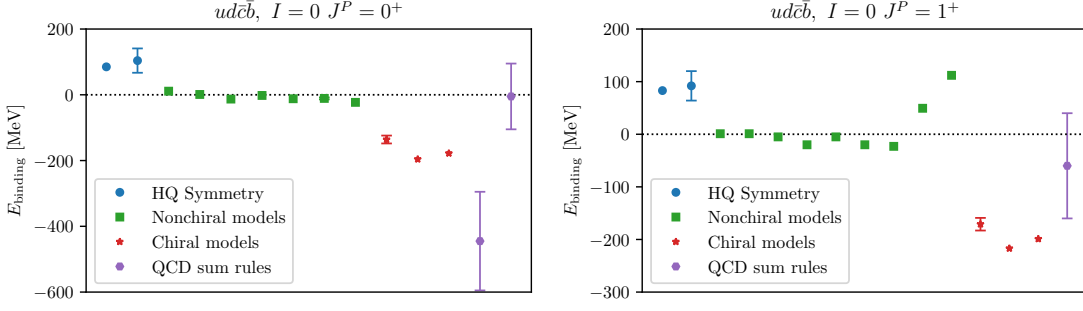


Figure 1: Various determinations of $I = 0, ud\bar{c}\bar{b}$ masses in the $J^P = 0^+$ (left) and $J^P = 1^+$ (right) channels. We show results from heavy quark symmetry, nonchiral models, chiral models, and from QCD sum rules.

1. Introduction

The existence of strong-interaction-stable, doubly-bottom tetraquarks with $J^P = 1^+$ has been firmly established in lattice QCD calculations [1–5]. These channels have light diquarks in a $\bar{3}_F$, spin 0 and colour $\bar{3}_C$ configuration, while the heavy anti-diquarks are in a colour 3_C , and with no spatial excitation are restricted to having spin 1. In the literature, various approaches have been used to study other tetraquark channels, and in some cases bound states have been predicted. We have focused on a selection of these channels where the light diquarks are in the same $\bar{3}_F$, spin 0 and colour $\bar{3}_F$ configuration as the established doubly-bottom channels, since from phenomenology it is known that this increases the chance of binding. The heavy anti-diquarks are similarly in a colour 3_C configuration. If the two antiquarks are the same then the anti-diquark can be in either a spin 0 or 1 configuration, while only spin 1 is possible if the two antiquarks are the same since we restrict our study to states without any spatial excitation.

We illustrate tetraquark mass results using these different methods in Figure 1. Here we limit this to $I = 0, ud\bar{c}\bar{b}$ channels with $J^P = 0^+$ and $J^P = 1^+$, and show the binding energy relative to the appropriate two-meson threshold. We also restrict these values to those that appeared in the literature in advance of the publication of ref. [6]. Results from heavy quark symmetry, nonchiral models, chiral models and QCD sum rules are depicted. Notice in particular the tension between the masses predicted by nonchiral models and chiral models. Despite the fact that both types of model were already fully constrained by fits to the ordinary meson and baryon spectrum, the chiral models predicted deep binding in these channels while the nonchiral models did not. Our lattice calculations can disambiguate the situation. A more thorough discussion of each channel of interest and a quantitative assessment of binding predictions is found in [6].

In these proceedings we briefly summarise the results of each channel, and provide an update on the status of doubly-bottom tetraquark binding energies having made improvements to our analysis methods.

2. Calculation details and lattice setup

We use the following set of operators that couple to tetraquark states with quark flavours ψ, ϕ, θ and ω :

$$\begin{aligned}
D(\Gamma_1, \Gamma_2) &= (\psi_a^T C \Gamma_1 \phi_b) (\bar{\theta}_a C \Gamma_2 \bar{\omega}_b^T), \\
E(\Gamma_1, \Gamma_2) &= (\psi_a^T C \Gamma_1 \phi_b) (\bar{\theta}_a C \Gamma_2 \bar{\omega}_b^T - \bar{\theta}_b C \Gamma_2 \bar{\omega}_a^T), \\
M(\Gamma_1, \Gamma_2) &= (\bar{\theta} \Gamma_1 \psi) (\bar{\omega} \Gamma_2 \phi), \quad N(\Gamma_1, \Gamma_2) = (\bar{\theta} \Gamma_1 \phi) (\bar{\omega} \Gamma_2 \psi), \\
O(\Gamma_1, \Gamma_2) &= (\bar{\omega} \Gamma_1 \psi) (\bar{\theta} \Gamma_2 \phi), \quad P(\Gamma_1, \Gamma_2) = (\bar{\omega} \Gamma_1 \phi) (\bar{\theta} \Gamma_2 \psi).
\end{aligned} \tag{1}$$

and select the largest basis providing numerically stable results for each tetraquark channel. Complete details of which combination of operators are used for each channel are again found in [6].

Using a matrix of correlators constructed from the above operators we next construct ‘‘optimized correlators’’,

$$C_i(t) = \sum_{j,k} V_{ij}(\tau)^\dagger C_{jk}(t) V_{ki}(\tau) \tag{2}$$

by solving a generalized eigenvalue problem (GEVP) [7–9]. The matrix V is constructed such that its columns are vectors v_j , which are the eigenvector solutions of

$$C_{ij}(t) v_j(t) = \lambda_i C_{ij}(t + t_0) v_j(t). \tag{3}$$

We choose the ‘diagonalization time’ [10], τ , such that projection onto the ground state is improved. To extract each of the energy levels of our tetraquarks, we perform a correlated single exponential fit to these correlators. The results presented in [6] and summarized in these proceedings use $t_0 = 2$ and $\tau = 4$. Although other choices are possible – and we find that the ground state masses are stable when these parameters are varied – larger values result in a deterioration of the statistical precision, which eventually leads to instabilities in the solutions.

For our calculations we use Wilson-clover ensembles with 2 + 1 quark flavours in the sea. All ensembles have a lattice spacing of $a^{-1} = 2.194(10)$ GeV. Pion masses range from $m_\pi = 700$ MeV down to 165 MeV. Two lattice volumes, $L^3 \times T = 32^3 \times 64$ and $48^3 \times 64$ are used. Those with a lattice volume of $32^3 \times 64$ were provided by the PACS-CS Collaboration [11]. The two $48^3 \times 64$ ensembles were generated by our collaboration. Details are given in Table 1. Only the lattice ensemble with $m_\pi = 192$ MeV is used for most of the results presented below, except for the update to the doubly-bottom channels reported previously in refs. [3] and [12], which uses all of the ensembles given here.

In the valence sector, the light and strange propagators use the Wilson-clover formalism as in the sea, although a slight mistuning of the strange sea quark means we use a partially quenched strange. For the charm propagators we use the Tsukuba interpretation of the Relativistic Heavy Quark action [13, 14]. We use a tadpole improved Nonrelativistic QCD (NRQCD) action for the bottom quarks with all Wilson coefficients, $c_i = 1$ [15].

3. Box-sinks

An important new feature of our analysis, and the principle improvement in our study of the doubly-bottom tetraquarks spectrum, is the box-sink construction that is implemented alongside Coulomb gauge-fixed wall sources [16, 17] that are fixed to high-precision using the Fourier-accelerated conjugate gradient algorithm [18]. In earlier work [3, 12], binding energy results came from correlators with local sinks. The use of local sinks with the Coulomb gauge-fixed wall sources

$L^3 \times T$	m_π [MeV]	N_{cnfg}	a^{-1} [GeV]
$32^3 \times 64$	700	399	2.194(10)
	575	400	
	415	400	
	299	800	
$48^3 \times 64$	192	122	
	165	88	

Table 1: Lattice volume, pion mass and number of configurations in each ensemble. There is a single lattice spacing: $a^{-1} = 2.194(10)$ GeV.

leads to correlators with negative signs for the amplitudes of (at least) the first excited states and ground-state effective mass plateaus which are approached from below. This can be of particular concern if the signal of the ground state does not last to large t , leading to poor plateaus. If instead a wall-sink is used, the ground state effective-mass plateau is approached from above, which is more desirable for avoiding possible overestimates of bound-state binding energies, but is also statistically noisy. To create such a ‘‘wall-wall’’ correlator, the wall-local propagators, $S(x, t)$, are summed over the spatial sites at the sink:

$$S^W(t) = \sum_x S(x, t). \quad (4)$$

The use of a box-sink ameliorates the negative features of both wall-local and wall-wall correlators discussed above. A box-sink is similar to a wall-sink except the wall-local propagators are summed over spatial sites residing within a sphere of radius R surrounding the reference sink point x :

$$S^B(x, t) = \frac{1}{N} \sum_{r^2 < R^2} S^B(x + r, t). \quad (5)$$

The choice $R^2 = 0$ then corresponds to a local sink and the maximum value, $R^2 = 3(L/2)^2$ is equivalent to a wall sink. This construction thus allows a continuous interpolation between these two extremes, permitting us to tune R^2 to obtain correlators whose effective masses approach their ground-state plateaus from above while not being hampered by unnecessarily large statistical noise. In Fig. 2 we demonstrate the use of box sinks on pseudoscalar B_c meson correlators, where the black circles correspond to a wall-local correlators, the blue triangles to wall-wall correlators, and the red and green squares correspond to wall-box correlators with $R^2 = 20$ and 49, respectively. In this case a box radius of $R^2 = 20$ would be the preferred choice owing to the long plateau.

4. Results

In Figs. 3, 4 and 5 we show the spectra of a number of channels obtained from the GEVP solutions. We find that the ground state energies are roughly consistent with the two meson thresholds. The exception is for both $\ell s \bar{c} \bar{b}$ channels (Fig. 4b) where the ground states lie slightly (< 10 MeV) below these thresholds. However, due to the lack of other nearby states, our suspicion is that this really corresponds to the two-meson threshold and the small apparent binding is due either

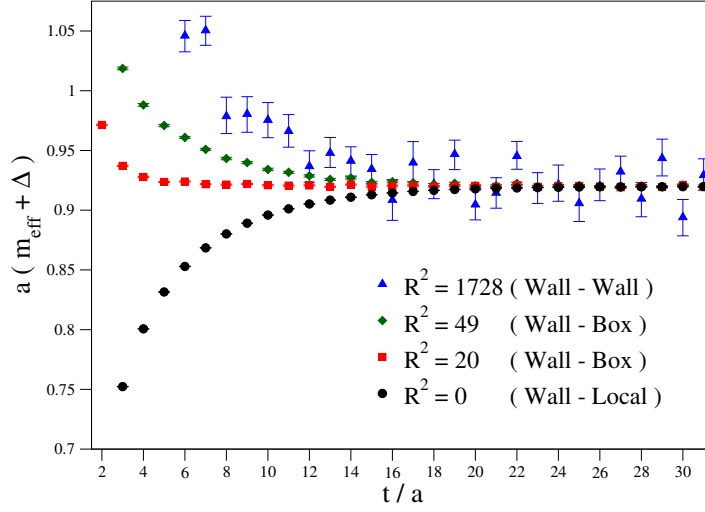


Figure 2: Effective masses for correlators describing the same B_c meson with different box-sink sizes R^2 in lattice units.

to a small finite volume effect or to another residual systematic in our analysis. Nevertheless, in all cases we can rule out the possibility of deep binding. The results are given in lattice units and other than in Fig. 3a, which shows absolute energies, the tetraquark energies are offset by an unknown quantity due to the NRQCD b quarks, but relative energies – and therefore binding energies – are preserved.

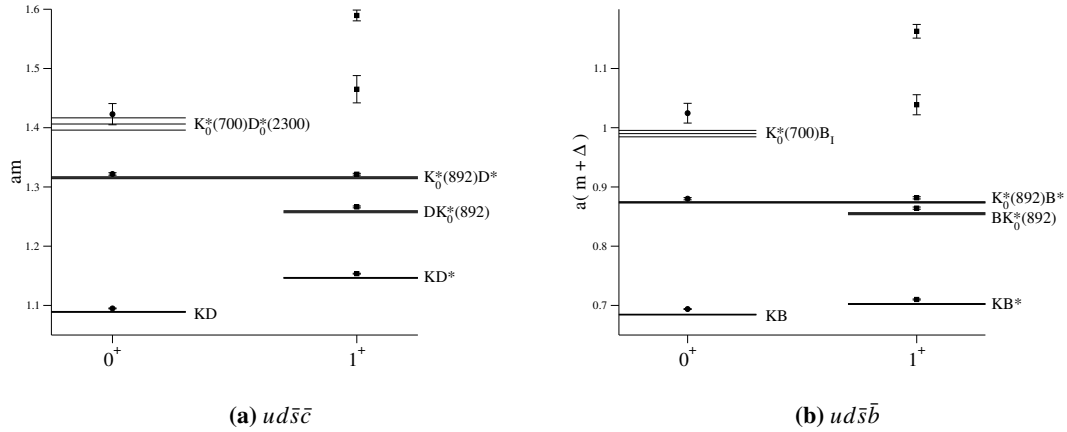


Figure 3: Fit results for the $I = 0$, $J^P = 0^+$ and 1^+ $ud\bar{s}\bar{c}$ (left) and $ud\bar{s}\bar{b}$ channels (right) alongside corresponding two-meson thresholds.

In Fig. 6 we provide a preliminary update of our results of the $J^P = 1^+ ud\bar{b}\bar{b}$ and $ls\bar{b}\bar{b}$ binding energies previously reported in [3]. The shaded band shows the extrapolation to the physical pion mass through a linear fit in m_π^2 with black points indicating results at physical pion mass. In agreement with the expected phenomenology, the binding energy increases as the light quark mass

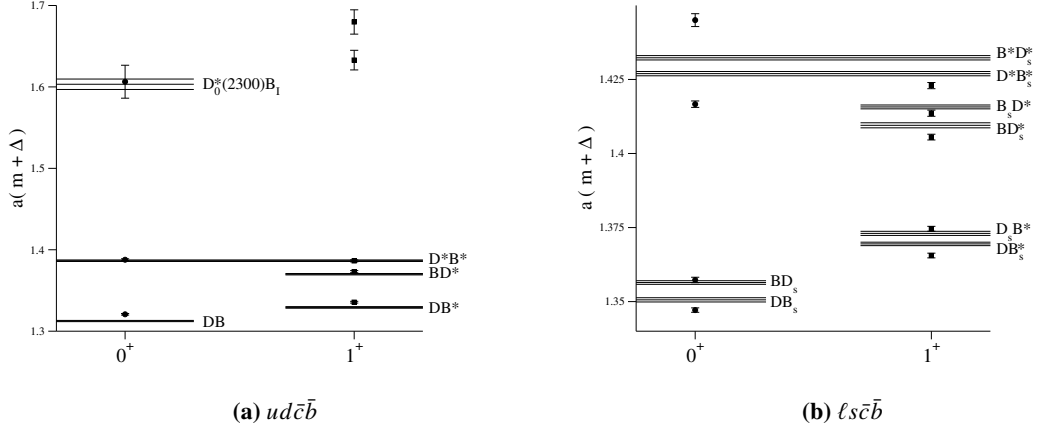


Figure 4: Fit results for the $I = 0, J^P = 0^+$ and 1^+ $ud\bar{c}\bar{b}$ (left) and $I = 1/2, J^P = 0^+$ and 1^+ $l s\bar{c}\bar{b}$ channels (right) alongside corresponding two-meson thresholds.

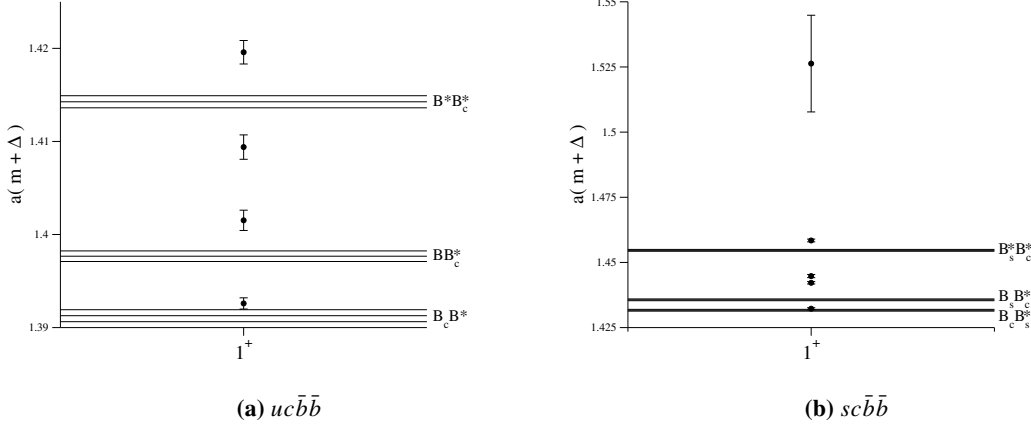


Figure 5: Fit results for the $I = 0, 1^+$ $uc\bar{b}\bar{b}$ (left) and $sc\bar{b}\bar{b}$ channels (right) alongside corresponding two-meson thresholds.

decreases. Each of the points as well as the extrapolated physical pion mass result show reduced binding compared with our previous values where a local sink was used. This demonstrates the importance of our wall-box correlators. Despite this difference, the qualitative conclusion remains the same: both the $I = 0, J^P = 1^+$ $ud\bar{b}\bar{b}$ and the $I = 1/2, J^P = 1^+$ $l s\bar{b}\bar{b}$ channels are strong-interaction stable. Indeed, the former remains comfortably below the BB threshold and is therefore also electromagnetically stable.

5. Conclusions

Using lattice QCD, we investigated tetraquark states that have been predicted as being bound and strong-interaction stable in studies that used QCD sum rules, model and/or heavy quark symmetry arguments. We have found evidence for deeply-bound, strong-interaction stable tetraquark states only in the doubly-bottom $J^P = 1^+$, $ud\bar{b}\bar{b}$ and $l s\bar{b}\bar{b}$, channels with $I = 0$ and $I = 1/2$, respectively.

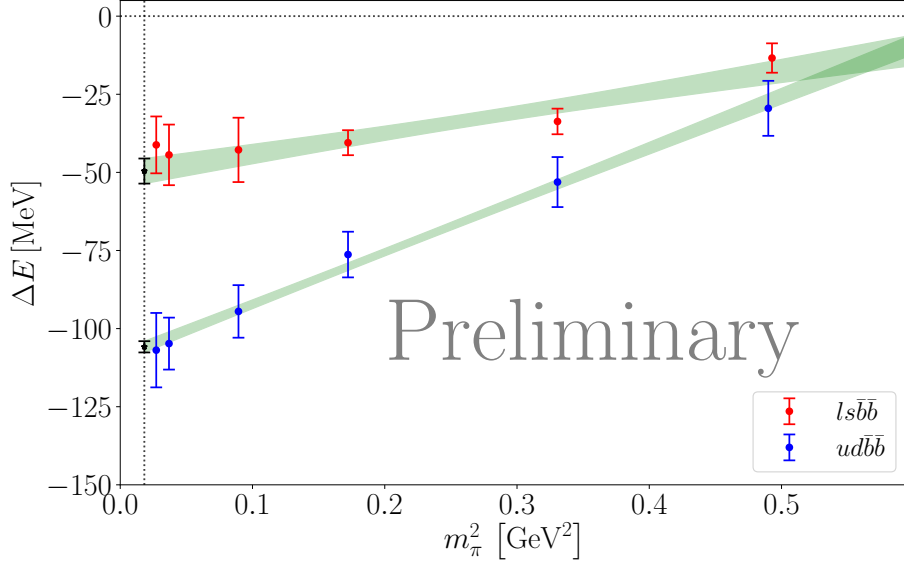


Figure 6: Linear extrapolation of the binding energies of the $J^P = 1^+ ud\bar{b}\bar{b}$ and $ls\bar{b}\bar{b}$ channels to physical light quark mass.

Deep binding in the other channels, as predicted by some model and QCD sum rules studies, would have been evident in this work but we found no such possibilities.

We are working on an update of the binding energies in the $J^P = 1^+, I = 0 ud\bar{b}\bar{b}$ and $J^P = 1^+, I = 1/2 ls\bar{b}\bar{b}$ channels. By using the box-sink construction we obtain an improved ground state signal and find that the binding energy for both states is somewhat reduced compared to our earlier work but still clearly strong-interaction stable. New gauge ensembles with lighter pion masses provide a more reliable extrapolation of the binding energies to the physical pion mass in both cases. An updated and extended study of doubly-bottom tetraquark channels is forthcoming.

Acknowledgments

B. C., R. L., and K. M. are supported by grants from the Natural Sciences and Engineering Research Council of Canada, R. J. H. by the European Research Council (ERC) under the European Unions Horizon 2020 research and innovation programme through Grant Agreement No. 771971-SIMDAMA. All computations were carried out using a crucial allocation from Compute Canada on the Niagara supercomputer at SciNet.

References

- [1] P. Bicudo, K. Cichy, A. Peters and M. Wagner, *BB interactions with static bottom quarks from Lattice QCD*, *Phys. Rev. D* **93** (2016) 034501 [1510.03441].
- [2] P. Bicudo, J. Scheunert and M. Wagner, *Including heavy spin effects in the prediction of a $\bar{b}\bar{b}ud$ tetraquark with lattice QCD potentials*, *Phys. Rev. D* **95** (2017) 034502 [1612.02758].

- [3] A. Francis, R.J. Hudspith, R. Lewis and K. Maltman, *Lattice Prediction for Deeply Bound Doubly Heavy Tetraquarks*, *Phys. Rev. Lett.* **118** (2017) 142001 [1607.05214].
- [4] P. Junnarkar, N. Mathur and M. Padmanath, *Study of doubly heavy tetraquarks in Lattice QCD*, *Phys. Rev. D* **99** (2019) 034507 [1810.12285].
- [5] L. Leskovec, S. Meinel, M. Pflaumer and M. Wagner, *Lattice QCD investigation of a doubly-bottom $\bar{b}\bar{b}ud$ tetraquark with quantum numbers $I(J^P) = 0(1^+)$* , *Phys. Rev. D* **100** (2019) 014503 [1904.04197].
- [6] R.J. Hudspith, B. Colquhoun, A. Francis, R. Lewis and K. Maltman, *A lattice investigation of exotic tetraquark channels*, *Phys. Rev. D* **102** (2020) 114506 [2006.14294].
- [7] C. Michael and I. Teasdale, *Extracting Glueball Masses From Lattice QCD*, *Nucl. Phys. B* **215** (1983) 433.
- [8] M. Luscher and U. Wolff, *How to Calculate the Elastic Scattering Matrix in Two-dimensional Quantum Field Theories by Numerical Simulation*, *Nucl. Phys. B* **339** (1990) 222.
- [9] B. Blossier, M. Della Morte, G. von Hippel, T. Mendes and R. Sommer, *On the generalized eigenvalue method for energies and matrix elements in lattice field theory*, *JHEP* **04** (2009) 094 [0902.1265].
- [10] B. Hörz and A. Hanlon, *Two- and three-pion finite-volume spectra at maximal isospin from lattice QCD*, *Phys. Rev. Lett.* **123** (2019) 142002 [1905.04277].
- [11] PACS-CS collaboration, *2+1 Flavor Lattice QCD toward the Physical Point*, *Phys. Rev. D* **79** (2009) 034503 [0807.1661].
- [12] A. Francis, R.J. Hudspith, R. Lewis and K. Maltman, *Evidence for charm-bottom tetraquarks and the mass dependence of heavy-light tetraquark states from lattice QCD*, *Phys. Rev. D* **99** (2019) 054505 [1810.10550].
- [13] S. Aoki, Y. Kuramashi and S.-i. Tominaga, *Relativistic heavy quarks on the lattice*, *Prog. Theor. Phys.* **109** (2003) 383 [hep-lat/0107009].
- [14] PACS-CS collaboration, *Charm quark system at the physical point of 2+1 flavor lattice QCD*, *Phys. Rev. D* **84** (2011) 074505 [1104.4600].
- [15] G.P. Lepage, L. Magnea, C. Nakhleh, U. Magnea and K. Hornbostel, *Improved nonrelativistic QCD for heavy quark physics*, *Phys. Rev. D* **46** (1992) 4052 [hep-lat/9205007].
- [16] A. Billoire, E. Marinari and G. Parisi, *COMPUTING THE HADRONIC MASS SPECTRUM. EIGHT IS BETTER THAN ONE*, *Phys. Lett. B* **162** (1985) 160.
- [17] R. Gupta, G. Guralnik, G.W. Kilcup and S.R. Sharpe, *The Quenched spectrum with staggered fermions*, *Phys. Rev. D* **43** (1991) 2003.
- [18] RBC, UKQCD collaboration, *Fourier Accelerated Conjugate Gradient Lattice Gauge Fixing*, *Comput. Phys. Commun.* **187** (2015) 115 [1405.5812].